24th COBEM - 2017

24th ABCM International Congress of Mechanical Engineering
December 3-8, 2017, Curitiba, PR, Brazil

COBEM-2017-1259
THE EFFECT OF WELDING CURRENT ON MECHANICAL STRENGTH OF RESISTANCE-SPOT WELDED TWIP STEEL SHEETS

Tiago Cristofer Aguzzoli Colombo
Guilherme J. dos Santos
Alfredo Rocha de Faria
Instituto Tecnológico de Aeronáutica. Department of Aeronautical and Mechanical Engineering. São José dos Campos, SP, Brazil.
colombo@ita.br, guilherme@ita.br, arfaria@ita.br
Vágner Braga
Luiz Fernando Rodrigues Junior
Centro Universitário Franciscano. Santa Maria, RS, Brazil.
vbraga@ita.br, luiz.fernando@unifra.br

Abstract. *Twinning-Induced Plasticity (TWIP) steels belong to the 2nd generation of Advanced High Strength Steels (AHSS). These steels combine unusual characteristics such as high yield strength, high ultimate strength and elevated ductility. However, the thermal cycles associated to the welding process during body-in-white manufacturing may change the metallurgical microstructure of these steels, thus affecting their mechanical strength and impairing their performance. This paper focuses on investigating the effects of welding current increments on the mechanical behavior of resistance spot welded TWIP steel sheets.*

Keywords: *Resistance Spot Welding, High-Strength Steels, Automotive Steels*

1. INTRODUCTION

The increasing demand for materials with higher performance for automotive industry has led to the development of innovative steel sheet grades with improved microstructure and mechanical performance, known as Advanced High Strength Steels (AHSS). The more complex metallurgy of AHSS grades provides a wide range of properties, combining strength levels with adequate ductility, especially when compared to other steel grades such as High Strength Low Alloy (HSLA) steels and non-ferrous alloys, such as Al, Ti and Mg alloys (Keeler, Kimchi and Mooney, 2017).

The Twinning-Induced Plasticity (TWIP) steels, which belong to the 2nd generation of AHSS, are good examples of such innovate steels. They exhibit yield strength and ultimate tensile strength levels above 500 MPa and 1GPa, respectively, combined with elongation values typical of low-C ferritic-perlitic steels (above 50% elongation) (Chiaberge, 2011; Bintu *et al.*, 2015). The versatility in mechanical properties added to their cold formability has gained attention to the automotive industry, as their use in body-in-white manufacturing may enhance strength and energy absorption of structural car body components during crash events.

However, the sophisticated physical characteristics of AHSS may be considerably affected by the thermal cycles associated to welding operations. For example, the localized heat input during welding processes may promote several metallurgical changes, such as grain coarsening, particles precipitation, recrystallization, etc. The typical high cooling rates may also promote phase transformations, both in the molten region as in the heat affected zones, which may also be accompanied by residual stresses (Blondeau, 2010; Zhang and Senkara, 2011). All these possible transformations may hence considerably affect the mechanical properties of the welded joint. In the light of the above, the aim of this work is to investigate the effects of the welding current on the quality, mechanical strength and energy absorption capacity of TWIP steel spot welds.

2. EXPERIMENTAL PROCEDURES

Uncoated cold rolled 0.8 mm thick Fe–Mn–C–Si–Al austenitic TWIP steel sheets supplied by POSCO (Pohang Iron and Steel Company, South Korea), with the chemical composition shown in Table 1, were considered in this study. Welding procedures were conducted using a Düring CB 150/560/76 kvA spot welding machine, under a constant electrode force of 2 kN, using a pair of copper electrodes with a face diameter of 6.0 mm. The electrodes were water cooled with a

constant flow rate of 6 L.min^{-1}. The welding current was divided into two different ranges: low heat input (4 kA to 7 kA) and high heat input (8 kA to 12 kA), with electrical current increments of 1.0 kA. All the other parameters were kept fixed such as presented in Table 2.

Chisel tests were performed to reveal the weld nugget and the interface between the individual sheets, in order to evaluate the appearance and the surface quality of the spot welds. In the chisel test, the spot weld is detached with aid of a hammer and chisel, exposing the weld nugget. This macroscopic analysis method is widely employed in the industry, and it is standardized by ISO 10447 (ISO, 2006).

Tensile-shear specimen were prepared following the AWS/SAE/D8.9 standard (American Welding Society, 2012). They were water jet cut in 50 x 30 mm dimensions oriented in the rolling direction and were welded by RSW linear overlapping positioned, as shown in Fig. 1. The tensile-shear properties of the spot welds were determined with a Instron 5500R/4206 Universal Testing Machine with a travel speed of 5 mm.min^{-1}. The tensile-shear maximum load, tensile-shear displacement and energy absorption at maximum tensile-shear load were analyzed and compared in order to investigate the effect of the welding current on these properties. The total energy absorption at maximum tensile-shear load was determined by numerical integration of the area under the tensile-shear load vs. displacement curves.

The nugget size was determined by micrograph analysis. The spot welds were cross sectioned along the centerline using a Isomet Low Speed precision cutter with the aid of a manual micrometer. The samples were then ground and polished by conventional metallographical procedures and etched with a 3% Nital solution for about 15s. Grain structure of the HAZ and BM was revealed by conventional metallographical procedure and etching with nital (4% HNO3) followed by chloridric acid (10%) and a solution of 10g of sodium metabisulfite (Na2S2O5) in 100 ml of distilled in water for 10 s.

The surface spot weld dimension and the indentation depth caused by electrode penetration during welding were measured using a Cyber CT-100 non-contact profilometer. Vickers microindentations were carried out on the metallographic samples across the fusion zone, HAZ and base metal 0.1 mm above centerline (sheet/sheet interface) under an indentation load of 1 N for 5s and with a spacing of 0.0625 mm between each indentation, according to ASTM E384 (ASTM International, 2016).

Table 1. Chemical composition and mechanical properties of the as-received TWIP steel sheets.

Chemical composition (%wt.)								
C	Mn	Al	Ti	Cr	Mo	Si	Ni	Fe
0.75	16.4	1.91	0.10	0.72	0.26	0.05	0.03	Bal.

Table 2. Welding parameters.

Parameter	Magnitude
Squeeze time	32 cycles
Welding time	8 cycles
Welding current	4 to 11 kA
Holding time	12 cycles
Electrode force	200 kgf
Sheet thickness	0.8 mm

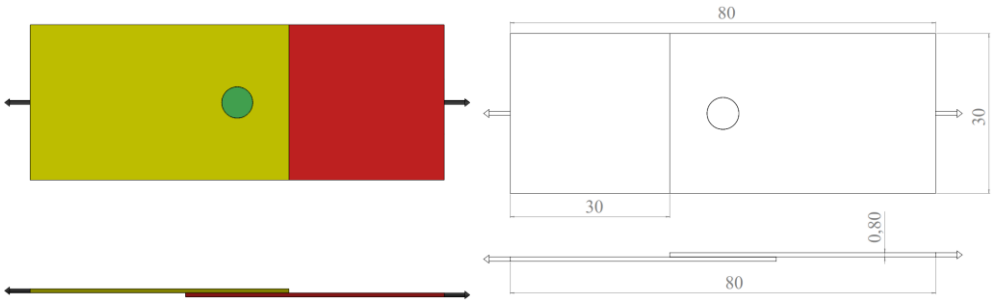

Figure 1. Schematic view of the tensile-shear test samples. Dimensions in mm.

3. RESULTS AND DISCUSSIONS

3.1 Macroscopic Aspects of the Spot Welds

Fig. 2 shows the influence of welding current on the spot weld quality and appearance. Welding current is a key factor directly associated to the surface quality of the spot welds, as excessive spatter and surface burn marks, which are typically originated from molten expulsion, may require costly rework to eliminate weld imperfections (Florea *et al.*, 2012). Such superficial imperfections were observed in the samples welded even with low heat inputs, as shown in Fig.2, evidencing that TWIP steels are prone to early molten expulsion. Severe molten expulsion and surface burn can be seen in the spot welds welded with 8 kA and above, indicating that high heat inputs may considerably impair the surface quality of the spot welds.

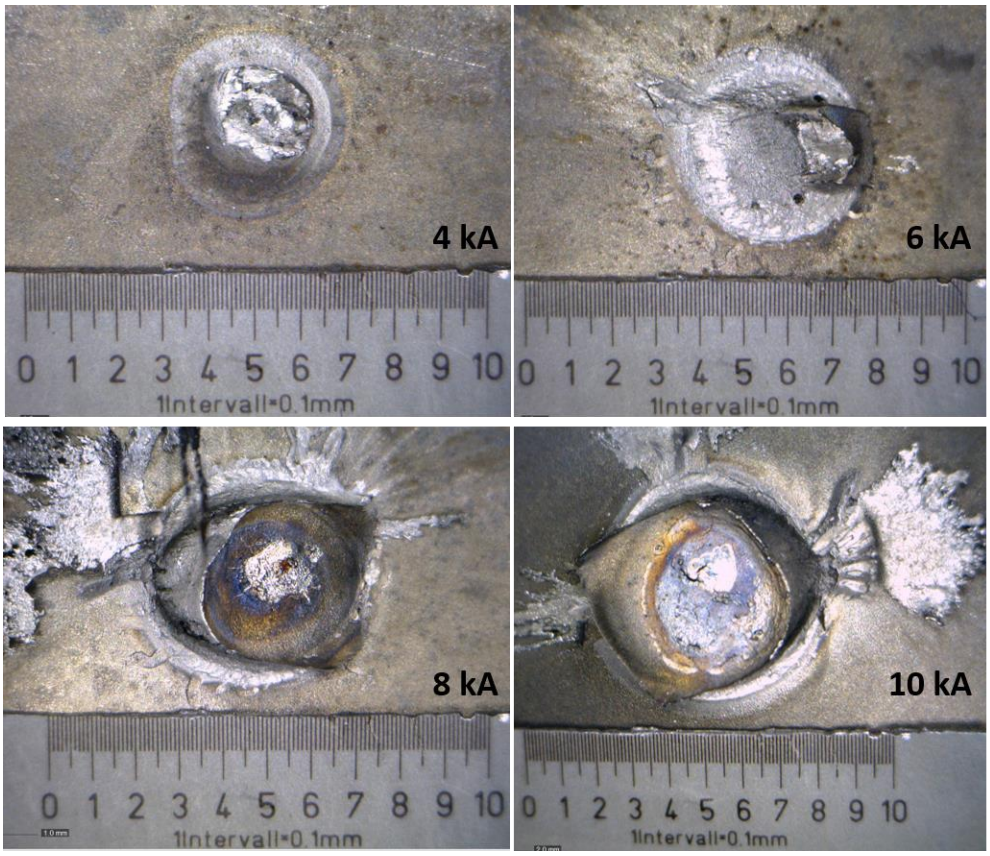

Figure 2. Spot weld appearances with different welding currents.

The geometrical attributes of spot welds are directly associated to the spot weld performance and they are used as reference to assess the spot weld quality and to compare different welding setups (Aslanlar, 2006). The nugget size and electrode indentation depth are the most used parameters to evaluate the quality of the spot welds. Fig. 3 (a) shows the spot weld and nugget growth curves. The nugget and spot weld size growth curves have similar behavior, exhibiting an increase in size with successive increments in welding current, especially above 7 kA, where it is possible observe am accentuated growth. Both spot weld and nugget have average sizes ranging between 3.4 and 4.0 mm when applying low heat inputs. For high heat inputs, the average sizes range between 4.7 and 6.0 mm. It is also possible to note from Fig. 3 (a) that the weld nugget size is slightly higher than the spot weld size. It is worth to note that both spot weld and nugget sizes tend to stabilize in 6.0 mm, which is the electrode tip diameter.

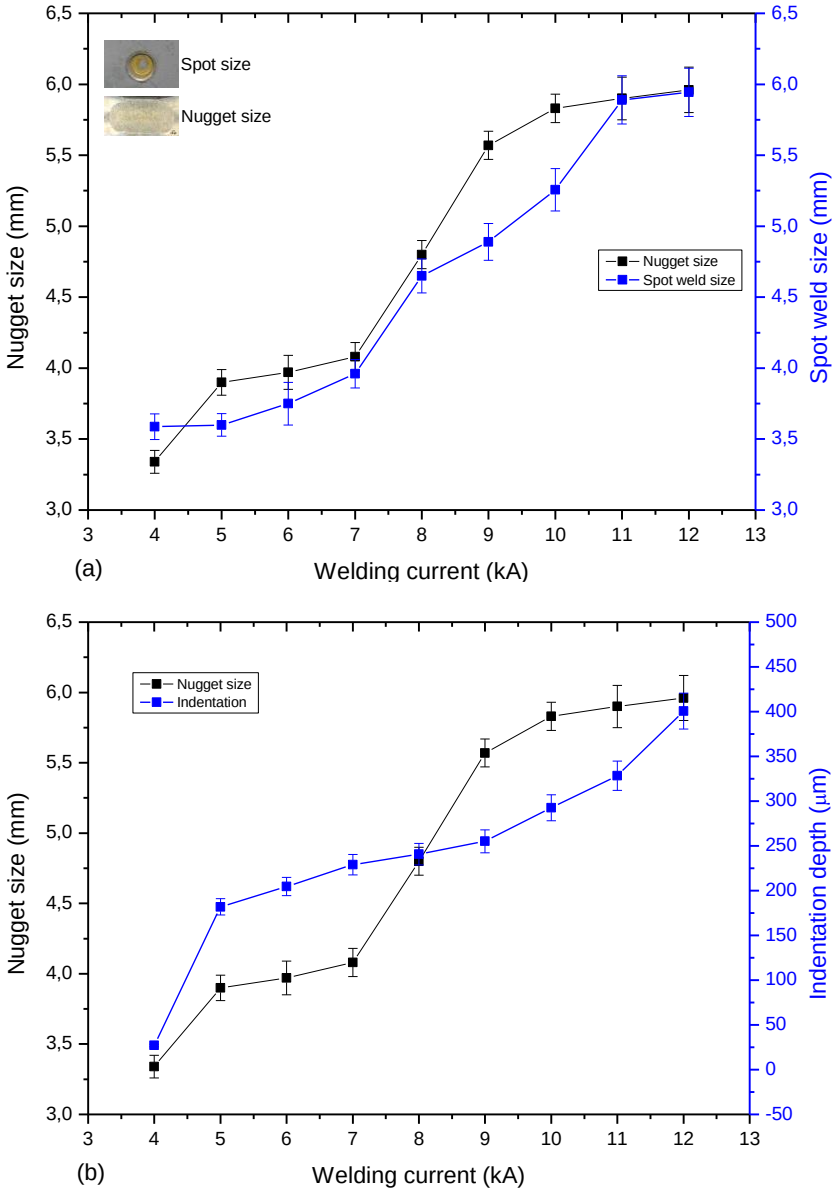

Figure 3. Geometrical attributes of the spot welds: (a) spot weld and nugget growth curves and (b) nugget and electrode indentation growth curves.

The larger the nugget size, the lower is the stress concentration along the weld nugget, which is beneficial to the mechanical strength of the spot weld. On the other hand, excessive electrode indentation depth may impair the mechanical performance of the spot weld, as the higher the electrode indentation depth, the smaller is the workpiece thickness, thus the smaller is the cross section that must withstand the mechanical loading, what may impair the load bearing capacity of the spot welds.

Fig. 3 (b) shows the nugget size and electrode indentation growth curves as a function of the welding current. The electrode indentation depth also tends to increase with increasing welding current. Shop floor practice in automotive industry and resistance spot welding recommendations in literature state a maximum electrode indentation depth value of 20% the workpiece thickness (Rautaruukki Corporation., 2009). Taking into account such considerations, the maximum acceptable electrode depth for a workpiece of 1.6 mm should be 320 μm, which corresponds to a maximum allowable welding current of 10 kA.

3.2 Microstructure

Fig. 4 shows the cross section of typical morphologies of a TWIP steel spot welds with a welding current of 8.0 kA. The morphology is the expected elliptic fused nugget formed between the two steel sheets, with a Heat Affected Zone (HAZ) around the nugget. The final solidification site locates in the geometrical center of the nugget, at the

sheet-to-sheet interface. The weld nugget has a symmetrical shape, due to the similarity in chemical composition and thickness between the individual steel sheets.

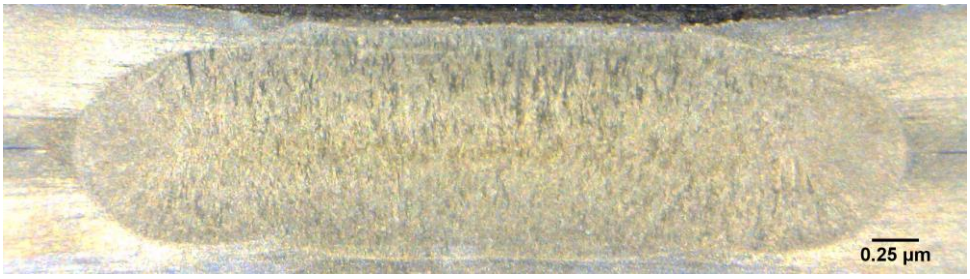

Figure 4. Nugget morphology of a TWIP steel spot weld. Welding current: 8 kA

It is possible to observe in Fig. 4 a typical dendritic grain structure at the Fusion Zone (FZ), with grain orientation normal to the weld center line, which is the last region to solidify. The grain orientation follows the heat dissipation, from the weld center line towards the electrodes, which are water cooled to force the cooling of the spot welds.

Fig. 5 shows the grain structure at the heat-affected zone (HAZ) and the base material (BM). The BM exhibits a very fine grain structure, with equiaxial grain with average size in the order of 2.5 µm. The HAZ is prone to considerable grain growth due to the high temperatures developed during the welding cycles. The average grain size at the HAZ is 15.6 µm, more than 6x the average grain size of the BM.

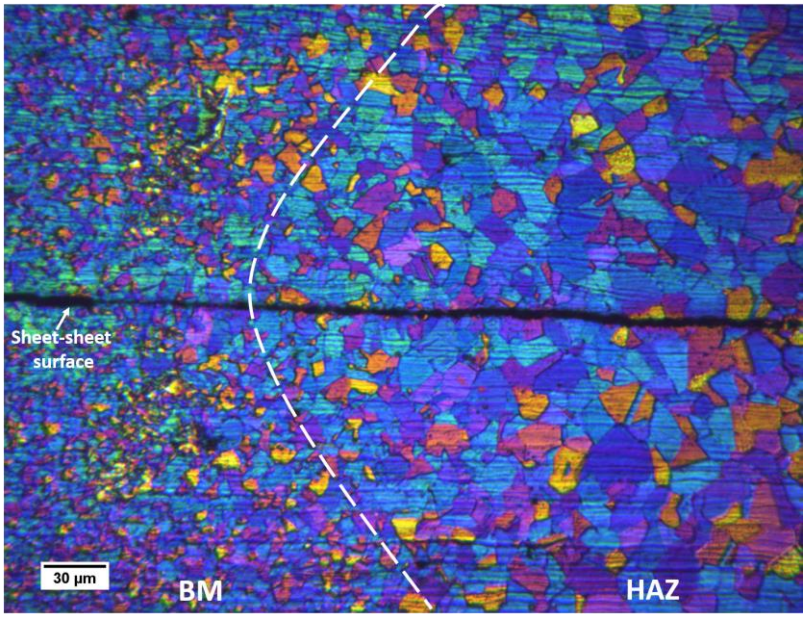

Figure 5. Optical micrograph of the grain structure at HAZ and BM. Welding current: 8 kA

3.3 Mechanical Properties

One of the major concerns when using AHSS for automotive applications is that the welding operations may impair the sophisticated post thermomechanical treatment metallurgy of these steels. Therefore, the load bearing capacity of the spot welds must be evaluated for a safe integration of new materials into a car body structure. Fig. 6 (a) shows the load bearing capacity of spot welds with low heat input levels. It can be seen that an increment of welding current provides both improvement on load bearing capacity and elongation. Spot welds with 4kA can withstand tensile-shear loads up to 4.1 kN, whereas spot welds using 7 kA can withstand tensile-shear loads up to 7.6 kN.

By applying high heat inputs (8 kA and above), it is possible to achieve higher load bearing and elongation values, as can be seen in Fig. 6 (b). Spot welds using 10 kA can withstand up to 9.1 kN with elongation values around 10 mm, more than 3 times the elongation capacity of spot welds using 7 kA. An increase in load bearing capacity and ductility is of great importance for body-in-white applications, as the energy absorption during collision events is directly related to the area under a tensile-shear load vs. elongation curves (Keeler, Kimchi and Mooney, 2017). By the tensile-shear load vs.

elongation curves in Fig. 6 (b) it can be seen that the severe molten expulsion accompanying high heat inputs did not seem to impair neither the nugget growth nor the mechanical performance of the spot welds.

The maximum load bearing capacity found was 9.75 kN, which is achieved with 12 kA. The results show that further welding current increments continue to promote an increase on load bearing capacity, which is accompanied by a higher elongation of the specimen at the maximum tensile-shear load, despite the high electrode indentation depth, which is higher than the maximum value recommended by industrial automotive practices, as discussed in Section 3.1. Therefore, such recommendations may not apply for TWIP steel spot welds, at least from a structural point-of-view.

The energy absorption is measured by numerical integration of the area under the tensile-shear load vs. elongation up to the maximum load, as highlighted in yellow in Fig. 7 (a), for a spot weld with 12 kA. Fig. 7 (b) shows the evolution of energy absorption capacity as a function of the welding current applied. It can be seen that the strengthening of the spot weld with the increase in welding current is accompanied by a considerable increase in energy absorption capability, especially when applying high heat inputs. These results show that welding current increments promote continuous strengthening of the spot welds, without impairing their plastic deformation ability up the maximum tensile-shear load.

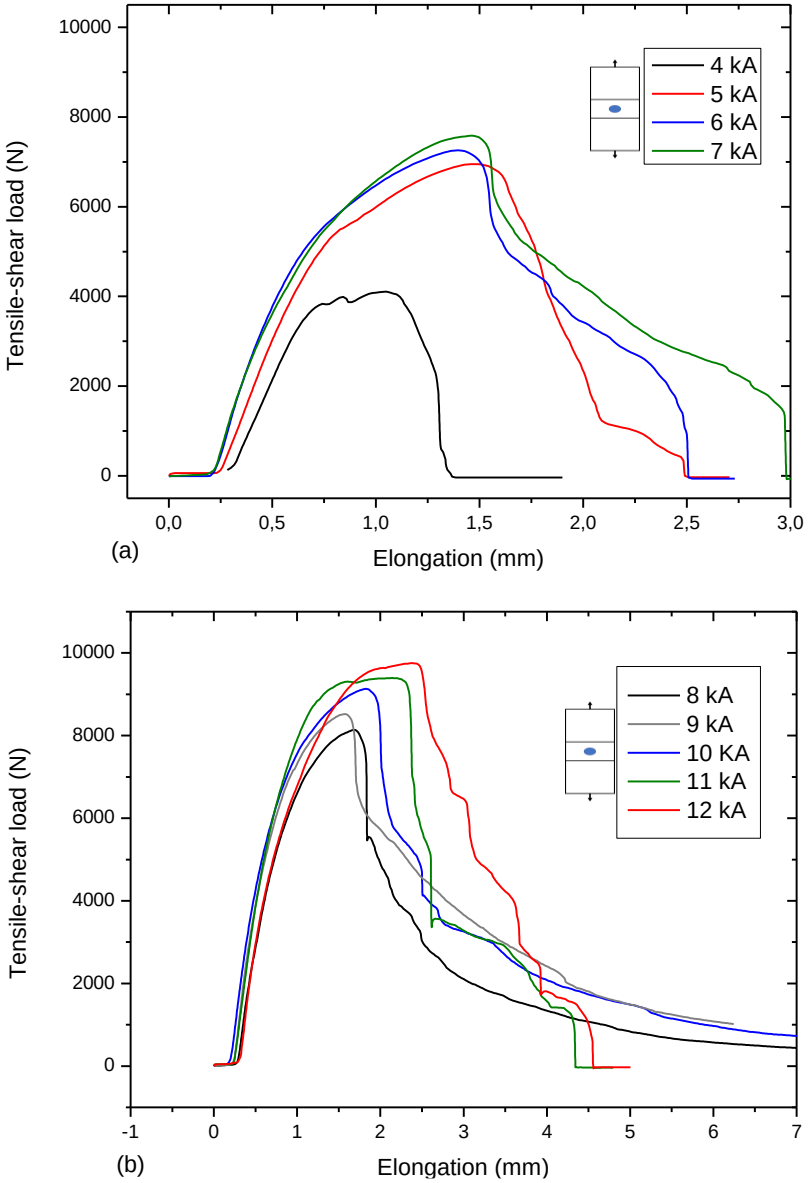

Figure 6. Tensile-shear load vs. elongation curves under different heat inputs:
(a) low heat inputs and (b) high heat inputs.

Fig. 8 shows the Vickers hardness profiles for spot welds with 6 kA and 8 kA. It is possible to observe that the hardness at the BM ranges from 267 to 300 HV, followed by a decrease in hardness at the HAZ towards the FZ. The decrease in hardness at the HAZ towards the FZ is justified by the grain coarsening observed at the HAZ, as shown in

Fig. 5. The hardness at the FZ ranges from 243 HV to 297 HV, with an average of 272 HV, slightly lower than the hardness at the BM.

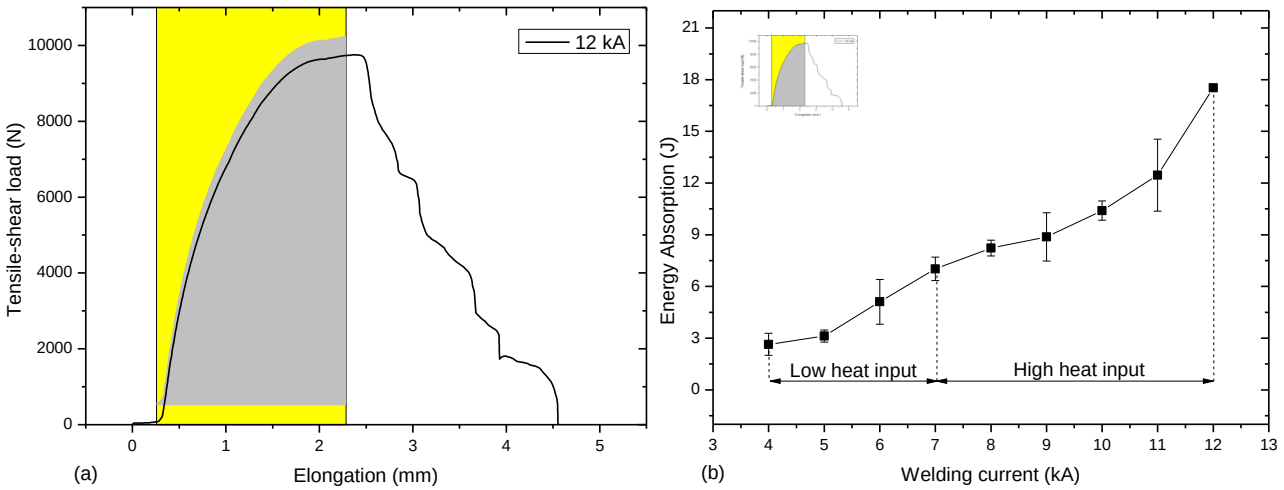

Figure 7. Tensile-shear load vs. elongation curves under different heat inputs: (b) low heat inputs and (b) high heat inputs.

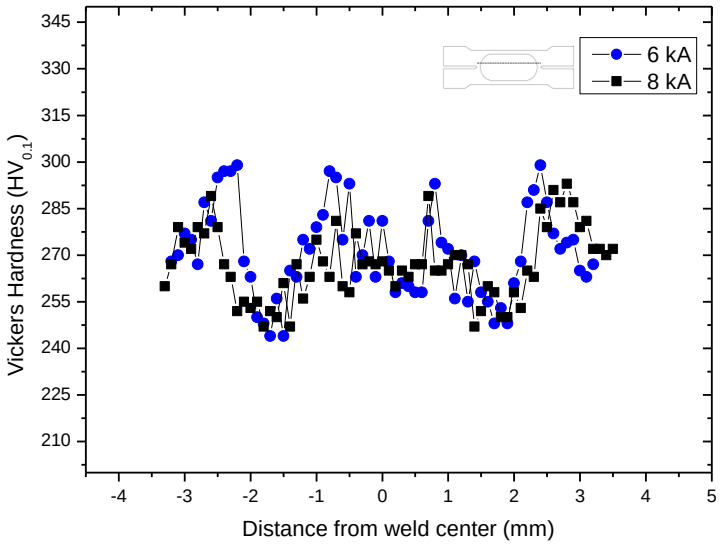

Figure 8. Vickers hardness profile for spot welds with welding currents of 6 kA and 8 kA.

Such results demonstrate that the rapid cooling does not seem to promote an increase in mechanical strength at the FZ. Similarly, an increase in welding current also does not seem to promote changes in mechanical strength of the HAZ and FZ, at least for the welding current range analyzed. Therefore, the increase in tensile-shear load and energy absorption with increasing welding current may be attributed solely to the increasing in weld nugget size.

The hardness values found at the HAZ and FZ are not in the range of the values expected for a martensitic microstructure, which indicates the efficiency of the Mn in stabilizing the austenitic phase of the studied TWIP steel, even when subjected to rapid heating and cooling cycles, as the ones found in resistance spot welding procedures.

However, as the hardness at the FZ is lower than the BM and HAZ, the absence of the weld button acting as a rigid body may facilitate the occurrence of fragile failure modes (interfacial failure) when the weldment is subjected to mechanical loading. Further investigations are needed to understand how the lower hardness at the FZ can influence the failure modes of the TWIP-TWIP spot welds.

4. CONCLUSIONS

The following conclusions can be drawn from the experimental results:

(1) TWIP steel resistance spot welds are strongly prone to molten expulsion, even when applying low heat inputs. High heat inputs tend to impair the surface quality by the occurrence of severe molten expulsion and surface burn.

(2) The weld nugget size is slightly higher than the spot weld size. Both nugget and spot weld size tend to increase with increasing welding current up to a welding current of 11 kA, then stabilizing at around 6.0 mm.

(3) Both load bearing capacity and elongation at the maximum tensile-shear load increase with increasing welding current. The maximum spot weld strength is achieved with a welding current of 12 kA. The same is observed for energy absorption, which increases with increasing welding current.

(4) The mechanical properties of the TWIP steel spot welds do not seem to be impaired by the excessive indentation depth cause by the welding electrodes.

(5) The hardness profiles show that the mechanical properties tend to decrease at the Fusion Zone when compared to the Base Metal, which implies that the increase in tensile-shear load and energy absorption with increasing welding current may be attributed solely to the increasing in weld nugget size.

5. ACKNOWLEDGEMENTS

Authors would like to acknowledge General Motors do Brasil and POSCO for suppling the materials used in this research. Additionally, the financial support provided by the Brazilian Federal Agencies CAPES and CNPq through grant 300886/2013-6 are gratefully acknowledged.

6. REFERENCES

American Welding Society, 2012. *Test methods for evaluating the resistance spot welding behavior of automotive sheet steel materials* (AWS Standard No. D8.9-12).

Aslanlar, S., 2006. "The effect of nucleus size on mechanical properties in electrical resistance spot welding of sheets used in automotive industry". *Materials and Design*, Vol. 27, p. 125–131.

American Society for Testing and Materials, 2017. *Standard Test Method for Microindentation Hardness of Materials (*ASTM Standard No. E384-17).

Bintu, A. *et al.*, 2015. "Strain hardening rate sensitivity and strain rate sensitivity in TWIP steels". *Materials Science and Engineering A*, Vol. 629, p. 54–59.

Blondeau, R., 2010. *Metallurgy and Mechanics of Welding: Processes and Industrial Applications*. John Wiley & Sons, New Jersey.

Chiaberge, M., 2011. *New trends and developments in automotive systems engineering*. InTech, Rijeka.

Florea, R. S. *et al.* 2012. "Resistance spot welding of 6061-T6 aluminum: Failure loads and deformation". *Materials and Design*, Vol. 34, p. 624–630.

Keeler, S., Kimchi, M. and Mooney, P. J., 2017. *Advanced High-Strength Steels Application Gudelines*. WorldAutoSteel Technical Report.

Rautaruukki Corporation, 2009. "Resistance Welding Manual". Rukki Metals Technical Report, p. 1–29.

Zhang, H. and Senkara, J., 2011. *Resistance Welding: Fundamentals and Applications*. CRC Press, Boca Raton, 2nd edition.

7. RESPONSIBILITY NOTICE

The authors are the only responsible for the printed material included in this paper.